ELSEVIER

Journal of Chromatography A, 849 (1999) 575–585

JOURNAL OF CHROMATOGRAPHY A

Salt effects in capillary zone electrophoresis IV. Resolution versus time and the effect of potassium phosphate and its concentration in the high ionic strength separation of sulphonamides

Reginald F. Cross*, Jing Cao

School of Engineering and Science, Swinburne University of Technology, John Street, Hawthorn, Victoria 3122, Australia

Received 28 December 1998; received in revised form 29 March 1999; accepted 10 May 1999

Abstract

The effects of potassium phosphate buffer and its concentration upon the capillary zone electrophoretic separation of 23 sulphonamides and a neutral marker were examined at pH 7. The resolution between the pairs was improved with the increased concentration of the buffer from 65 m*M* to 174 m*M*. Nineteen sulphonamides, a hydrolysis product and several unidentified minor components were baseline resolved in both 101 and 138 m*M* phosphate buffers. In 174 m*M* buffer all 21 ionised sulphonamides and the other compounds were separated. A simple relationship between the resolution of analyte pairs (R_s) and the square root of the mean analysis time for the pair ($\sqrt{t_{app}}$) was derived, but few of the pairs displayed this behaviour. For the majority of pairs of compounds, Joule heating appeared to cause a maximum in the R_s versus $\sqrt{t_{app}}$ relationship, while non-ideality and shifts in ionisation with increasing salt concentration appeared dominant in other cases.

Keywords: Salt effects; Resolution; Buffer composition; Sulphonamides

1. Introduction

There have now been several investigations of the separation of a significant number of sulphonamides (SFAs) by capillary electrophoretic techniques, eight by capillary zone electrophoresis (CZE) [1–8] and two by micellar electrokinetic chromatography [9,10]. The specific structures of the SFAs have been written in several places, and for the extended set that we have used, may be found in Refs. [3,7]. The general structure is shown in Fig. 1.

According to the structures and thus ionisation reactions, the SFAs are divisible into three categories. Each has two ionisable groups and the majority of pK_a data may be found in Refs. [2–4,7].

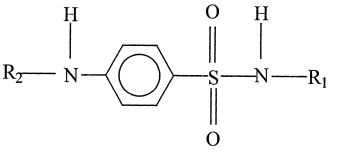

Fig. 1. General structure of sulphonamides.

*Corresponding author. Tel.: +61-3-9214-8578; fax: +61-3-9819-0834.

E-mail address: rcross@lucy.swin.edu.au (R.F. Cross)

0021-9673/99/$ – see front matter
PII: S0021-9673(99)00627-5

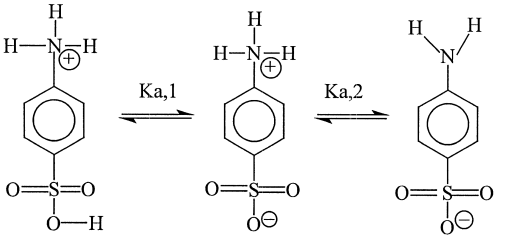

Fig. 2. Dissociation equilibria of sulphanilic acid (category 1).

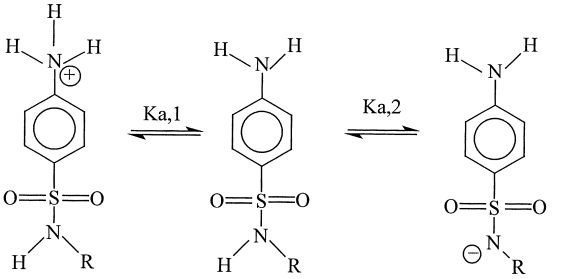

Fig. 4. Dissociation equilibria of category 3 sulphonamides.

Sulphanilic acid (SA) is unique amongst the analytes and comprises the first category (R_1 and R_2 = H) (see Fig. 2). It is both protonated on the anilinic group and ionised on the sulphonic acid site around pH 2 [at the lowest pH values of interest for analysis whether by capillary electrophoresis (CE) or high-performance liquid chromatography (HPLC)]. This zwitterion is progressively converted to the anionic form with increasing pH ($pK_{a,2}$ = 3.2).

The second category of SFAs is made up of those containing both carboxy amide (R_2 = succinyl or phthalyl) and sulphonamide (R_1) groups. These are anionic at lower pH values and di-anionic around neutral to higher pH values (see Fig. 3).

The third category comprises the majority of the SFAs. R_2 = H so that these analytes are cationic at low pH values, electrically neutral at intermediate pH values and are anionic at higher pH values (see Fig. 4).

Hence the choice of pH for CZE analysis is dependent upon the particular analytes. Most studies [1–4,6,7] have chosen the higher pH range (where each category of SFA is anionic) and have used the conventional CZE configuration in which the analytes follow the neutral marker (and hence allow for the maximum separation time and space [11]). This

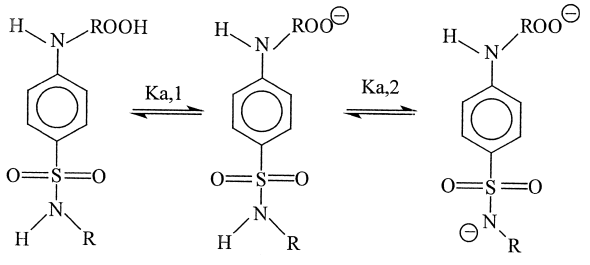

Fig. 3. Dissociation equilibria of sulphonamides forming doubly charged negative ions (category 2).

has been particularly appropriate both for the large set of SFAs we have examined (23) [3,7] and for the fast separations that have been done on the 13 SFAs chosen from a set of 16 [4,6]. Where the pH has been optimised, values very close to 7 have been obtained in each case [1–4,6]. The only shortcoming of the above strategy is that sulphanilamide (SAA) and sulphaguanidine (SGW) have $pK_{a,2}$ values that are too high for any significant ionisation to occur at pH 7. However, it has been found that SGW can be separated from the neutral marker in spite of this [7] so that SAA is the single problematic analyte. The alternative approach is to choose a low pH [5,8] where the SFAs of the third category are all cationic. This has the advantage of including SAA and SGW as ionic species, but renders the second category of SFAs (anions at low pH) unanalysable as there is no electroosomotic flow (EOF). Also, the zwitterionic SA will not be separated from electrically neutral components. Lin et al. [5] have utilised pH 2 to essentially separate their full set of 16 third category SFAs, albeit in 45 min.

In our first CZE study involving the screening of a large number of SFAs [3], improved separations were indicated in the higher concentrations of the (mixed sodium/potassium) phosphate buffer utilised. Then high concentrations of the running buffer were confirmed as a powerful tool with the eventual achievement of the difficult separation of the final pair of dihydrofolate reductase inhibitors [12] in sodium phosphate buffers. This is consistent with the work of Janini et al. [13], and others. Hence the use of highly concentrated sodium phosphate buffers in our last study of the separation of the SFAs [7]. Improved separations were achieved, but the differences in selectivity noted [7] between the use of a

mixed sodium–potassium buffer [3] and the single sodium salt [3] indicated that the single potassium salt might yield even better resolution of all pairs. This is strongly supported by the results of Issaq et al. who have demonstrated the systematic improvement in resolution as the size of the bare alkali metal cation in the buffer is increased [14]. Hence it is logical to investigate the separation of the SFAs in concentrated potassium phosphate buffers.

On the other hand, in an earlier study by Isaaq et al. [15], it was found that resolution was better in sodium phosphate buffers than potassium phosphate buffers. Interestingly, the authors did not comment on this apparent inconsistency between their papers [14], but, assuming both sets of data to be correct, since the same dansyl amino acids were used in each case, the implication is that the buffer anion modifies the behaviour of the cation. (The later study used acetate buffers [14]). However, it is possible that the SFAs are affected by the buffer cation in a manner different to that of the dansyl amino acids.

2. Theory

The operational definition of resolution is given by Eq. (1):

$$R_s = \frac{\Delta t_{app}}{\frac{1}{2}(w_1 + w_2)} \quad (1)$$

where the apparent migration time (or time of emergence) is t_{app} and the w are peak widths. Assuming there is no Joule heating and that longitudinal diffusion is the only mechanism of band broadening, then [11] the spatial variance in the zone width of the analyte (σ^2) is given by:

$$\sigma^2 = 2Dt_{app} \quad (2)$$

With $w = 4\sigma$:

$$R_s = \frac{t_{app}(2) - t_{app}(1)}{2\sqrt{2}\left[\sqrt{D_1 t_{app}(1)} + \sqrt{D_2 t_{app}(2)}\right]}$$

Defining $\overline{t_{app}}$ as the mean apparent migration time for two analytes and $f(\overline{t_{app}})$ as the function relating the position of the individual analytes to the mean position for the pair and simplifying:

$$R_s \approx \frac{\sqrt{\overline{t_{app}}}\left[f(\overline{t_{app}},2) - f(\overline{t_{app}},1)\right]}{2\sqrt{2}\cdot\left[\sqrt{f(\overline{t_{app}},1)D_1} + \sqrt{f(\overline{t_{app}},2)D_2}\right]} \quad (3)$$

For any series of separable analytes, there must be some intrinsic electrophoretic difference(s) such as charge or size and the $f(\overline{t_{app}})$ will thus be analyte specific. However, to a first approximation Eq. (3) shows that:

$$R \propto \sqrt{\overline{t_{app}}} \quad (4)$$

For a fixed field strength, any variation in experimental conditions that prelongs a CZE analysis by a decrease in μ_{ep}, and consequential increase in $\sqrt{\overline{t_{app}}}$, should lead to increased resolution.

Of the many variables that may be used to slow down CZE analyses and allow greater time for discrimination between analytes, pH is the most powerful (and potentially the most discerning). Decreased pH can reduce the EOF by more than an order of magnitude. However, when the pH is optimised but full separation is not achieved, a choice has to be made of which other variable to utilise. Lowering the temperature [16], introducing an appropriate organic modifier [17] and increasing the buffer concentration [3,7,12,13,15] are all within the domain of CZE and readily achieved.

3. Experimental

3.1. Instrumental

A Model 270A CE System by Applied Biosystems (Foster City, CA, USA) was used for all CZE experiments. The analytes were detected by UV absorbance at 254 nm and the detector time constant was set at 0.3 s in all experiments.

Separations were performed at 30°C with 18 kV applied to a 67.3 cm×50 μm I.D.×220 μm O.D. fused-silica capillary (Applied Biosystems) with the detection window located 49.0 cm from the injection end. Vacuum injection took place at the anode (+).

3.2. Chemicals and materials

Standard stock solutions of each compound were prepared by precisely dissolving 0.1 g in 100 ml of HPLC grade methanol (BDH). Each compound was diluted with Milli-Q water to give a final concentration of 25 ng/μl. Sample solutions were filtered (0.45 μm) before injection. The potassium phosphate buffer concentrations were 65 m*M* with respect to phosphate ($\sqrt{I}=0.339$, where I is the ionic strength), 101 m*M* ($\sqrt{I}=0.423$), 138 m*M* ($\sqrt{I}=0.492$), and 174 m*M* ($\sqrt{I}=0.553$), and were prepared from K_2HPO_4 and KH_2PO_4 after calculation of the exact amounts required. Precise masses were then dissolved, the solutions magnetically stirred and the stable pH recorded. Where the pH was slightly outside of the range of 7.00 ± 0.05, a small number of drops of 20% H_3PO_4 or 0.1 *M* KOH were added to obtain the desired pH of 7.0.

Compound 1 is the neutral marker. This was provided by the 4% methanol present in the stock solution of SFAs and caused a clear baseline disturbance (refractive index variation) when passing through the detector. The sulphonamides used in this study, their abbreviations used in the text and the numbers used to label them in the figures are: sulphanilamide (SAA, 2), sulphaguanidine (SGW, 3), sulphapyridine (SPYR, 4), sulphamethazine (SMZ, 5), sulphisomidine (SISM, 6), sulphamoxole (SMO, 7), sulphamethoxypyridazine (SMOP, 8), sulphathiazole (ST, 9), sulphamerazine (SMR, 10), sulphameter (SME, 11), hydrolysis product (HP), sulphadimethoxine (SDIM, 12), sulphadiazine (SDI, 13), sulphaquinoxaline (SQ, 14), sulphachloropyridazine (SCP, 15), sulphabenzamide (SBE, 16), sulphamethoxazole (SMOZ, 17), sulphisoxazole (SIOX, 18), sulphamethizole (SMI, 19), sulphacetamide (SAC, 20), phthalyl sulphathiazole (PST, 21), succinyl sulphathiazole (SST, 22), phthalyl sulphacetamide (PSAC, 23) and sulphanilic acid (SA, 24). They were obtained from Sigma (St. Louis, MO, USA). The structures of all of the SFAs are given in Ref. [7].

3.3. Methods

Capillary preparation at the start of each day of experimentation involved initial purging with 0.1 *M* NaOH for 3 min, followed by Milli-Q water purging for 3 min and then the running buffer for 3 min. Between runs, the capillary was purged with 0.1 *M* NaOH for 3 min followed by running buffer for 3 min. Vacuum injections of 7 s duration were used. At the nominal 4 nL per second specified by the manufacturer, 28 nl would have been injected. However, the more viscous buffers used would lead to greatly reduced injection volumes. Furthermore, as the sample was dissolved in water, sample stacking compensated for this larger than usual volume.

4. Results and discussion

4.1. Separations and resolution

In choosing the concentrations of potassium phosphate buffer for this study, we were mindful of the buffer concentration ranges that had yielded the most promising results in earlier studies [3,7,12]. However, the highest concentration of (sodium phosphate) buffer used in the previous study [7] (210 m*M*) gave rise to excessively high noise when utilised with the potassium buffer and so was not pursued. This may have been due to the higher conductivity of the potassium salt.

Fig. 5 is a plot of t_{app} versus $\sqrt{I}$. It serves to demonstrate the systematic spreading of all pairs of ionised analytes. In this regard, the data are generally similar to those obtained in sodium phosphate buffers (7). However, in this case the exact shapes of the curves are ambiguous, presumably due to experimental error. If it is the second set of data (101 m*M* buffer, $\sqrt{I}=0.423$), that is too high-lying, then the deviation from linearity is similar in both the potassium and sodium phosphate buffers. To investigate this further, we have again split the data into its two component parts (Fig. 6). The plot of the variation in the electroosmotic mobility shows a minimum at the second highest value of $1/\sqrt{I}$ (second lowest value of $\sqrt{I}$) which is logically unexpected and inconsistent with both our data in sodium phosphate buffers [7] and with the data of others [18]. It must therefore be concluded that there was some unsystematic variation in the condition of the capillary surface after preparation for that set of

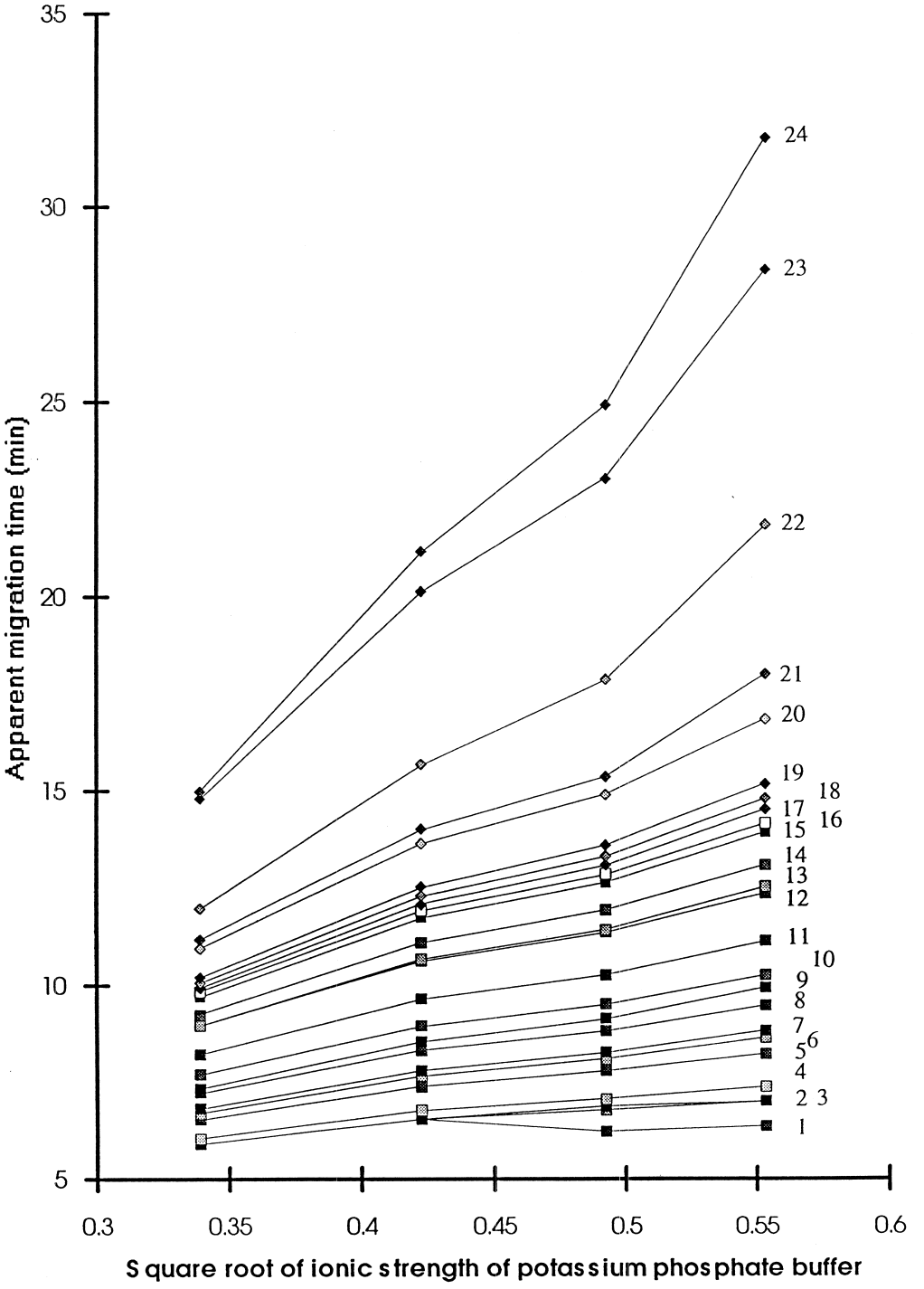

Fig. 5. Apparent migration times of the neutral marker (1) and 23 SFAs (min) versus the square root of the concentration of the sodium phosphate buffer (m*M*). For details see Experimental.

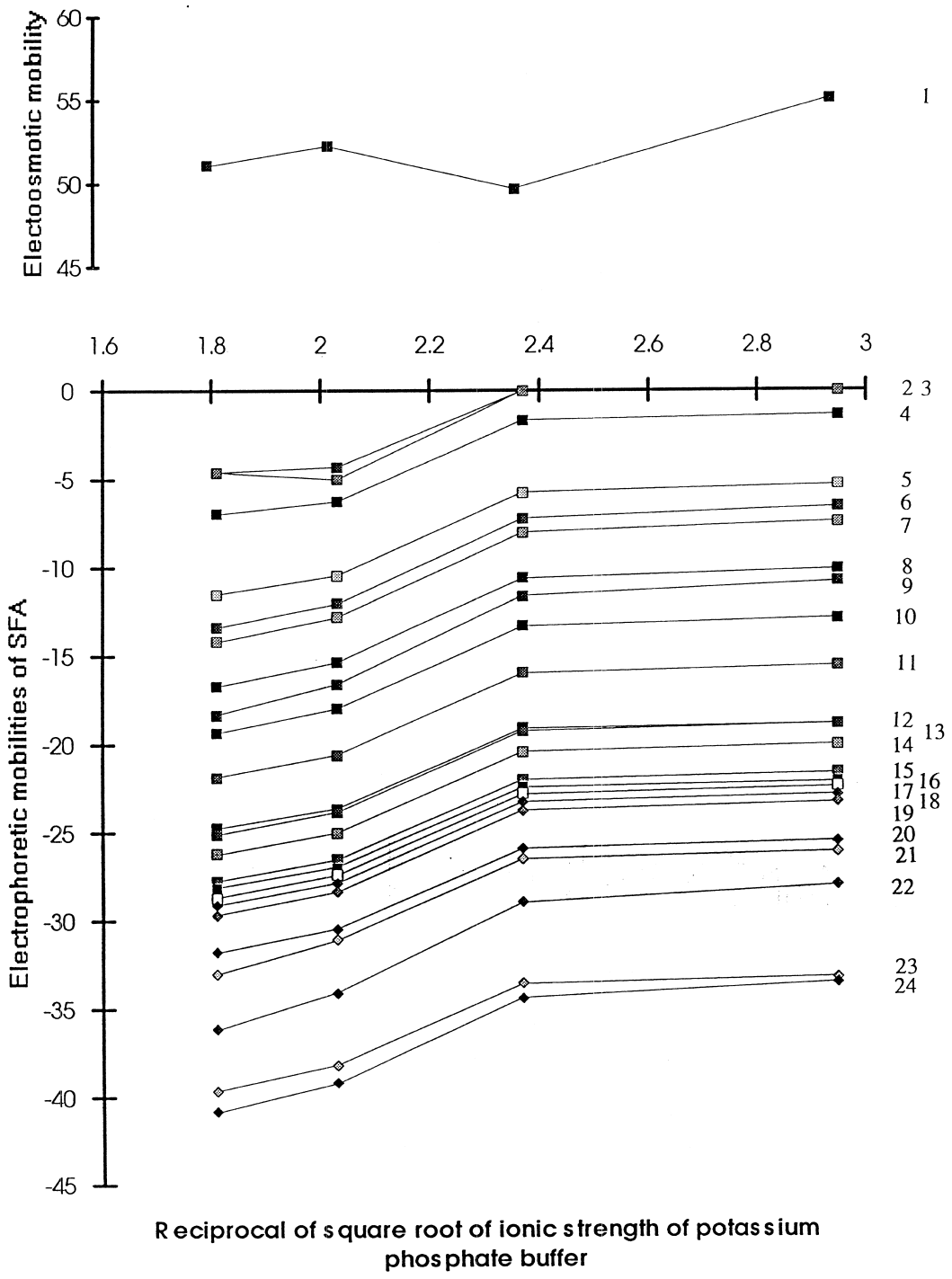

Fig. 6. The electroosmotic mobility as measured by the neutral marker and the electrophoretic mobilities of the 23 SFAs, all plotted versus the reciprocal of the square root of the ionic strength of the potassium phosphate buffer. For details see Experimental.

experiments. Assuming that to be the case, an approximately linear variation of t_{app} versus $\sqrt{I}$ would be obtained at low $\sqrt{I}$ in Fig. 5, with deviation at high $\sqrt{I}$, as expected. However, the disadvantage of the method of data presentation in Fig. 5 is that peak widths are not taken into account.

Fig. 7a–d shows the electropherograms obtained in the 65, 101, 138 and 174 m*M* potassium phosphate buffers, respectively. Note that the electropherograms have been scaled to fit the width of the page in each case. This places each peak approximately the same distance across all electropherograms and permits a direct comparison of relative separations and peak widths. As resolution [Eq. (1)] is a direct ratio of the separation (time or distance) to the mean peak width (time or distance), this facilitates ready visualisation of the relative resolutions obtained in each electropherogram. Several examples of improved resolution with increasing buffer concentration (and thus time of analysis, t_{app}) are immediately apparent. SFA pairs 8/9, 20/21 and 23/24 all clearly show improved resolution from chromatograms a–d. Similarly, the unidentified compound causing the fronting on SFA 22 in electropherogram (a) is obviously baseline resolved in (b) and greatly further resolved in electropherograms (c) and (d). Of greater interest, however, are the resolutions of the SFA pairs 16/17 and 12/13 with increasing salt (buffer) concentrations. The group of compounds 15–19 are often not resolved [3,7] and it is unfortunate that sulphabenzamide (16) was not included in the work of Lin and co-workers [4–6] and that sulphamethizole (19) was only included in one of these studies [5]. In the case of SFAs 15–19, the best resolution appears to be around 138 m*M* for the potassium phosphate buffer. Clear loss of resolution occurs when the buffer is increased to 174 m*M*, although the apparent peak distortion of 15 is not real. (Blowing up the electropherogram shows peaks 15 and 16 to be symmetrical and have $R_s \approx 1.1$, compared to about 1.25 in the 138 m*M* buffer). Peaks 12 (sulphadimethoxime) and 13 (sulphadiazine) comigrate in 65 and 101 m*M* buffer (Fig. 7a and b), begin to separate in 138 m*M* buffer (Fig. 7c) and are largely resolved ($R_s \approx 1.1$) in 174 m*M* buffer (Fig. 3d).

The best separation is achieved in the highest concentration buffer, at 174 m*M* potassium phosphate (Fig. 7d). All of the 21 ionised SFA are separated, with the least resolved pair being compounds 15 and 16 ($R_s \approx 1.1$). In addition, the remaining two compounds (2 and 3) are largely separated from the neutral marker.

At the start of the electropherogram in Fig. 7a the neutral marker (NM, 1), sulphanilamide (SAA, 2) and sulphaguanidine (SGW, 3) appear to form a more structured band than the featureless ''blob'' previously observed in sodium phosphate buffers [7]. Fig. 7b–d show a slight improvement of this definition as the buffer concentration increases and clearly indicate differentiation from the NM. Whilst this also occurred to some degree in the sodium buffer, the extent of separation in the potassium salt is far more pronounced. As previously pointed out [7], with $pK_{a,2}$ values of 10.4 and 11.3, respectively, the electrophoretic mobilities of SAA and SGW would be negligible at pH 7, even for an order of magnitude shift in the ionisation, which might be caused by non ideality in concentrated buffers [7]. Thus some other mechanism of differentiation appears to be operative. Adsorption again seems most likely.

4.2. Resolution versus time

While obvious increases in resolution can be observed from Fig. 7 and have been pointed out in the previous section, in most instances it is more difficult to gauge changes in resolution of pairs of analytes. The data in Fig. 5 is not helpful because peak widths are absent. According to the simplified Eq. (4), a linear relationship should exist between R_s and $\sqrt{t_{app}}$. On the other hand, Eq. (3) indicates a more complex relationship. Fig. 8 shows plots of R_s versus $\sqrt{t_{app}}$ $(=t^{1/2})$ for all pairs of analytes for which meaningful measurements of the peak width at the half-height ($w_{1/2}$) could be made. The measurements were made manually from photo-enlarged copies of the electropherograms and R_s was calculated from Eq. (1), modified by $w = 4w_{1/2}/2.354$.

For the pairs of compounds that appeared to obviously experience increased resolution with increasing buffer concentration in Fig. 7, the confirmation can be seen in Fig. 8. Pairs 8/9 and 16/17 in Fig. 4a and pairs 20/21 and 23/24 in Fig. 4b all display continuous increases in R_s, although in the

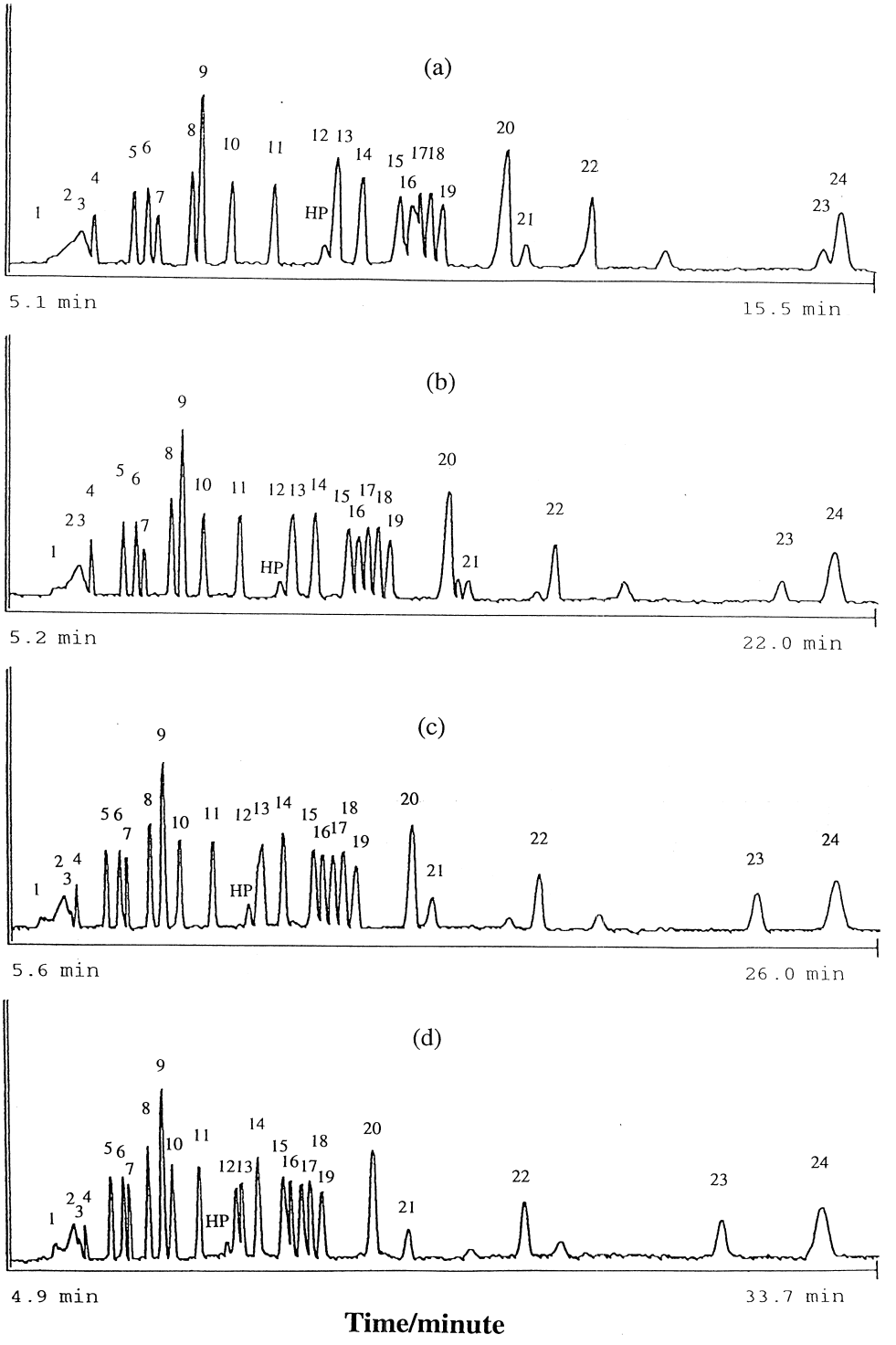

Fig. 7. Electropherograms of the SFAs in potassium phosphate buffers (a) 65 m*M*, (b) 101 m*M*, (c) 138 m*M*, (d) 174 m*M*. For details see Experimental.

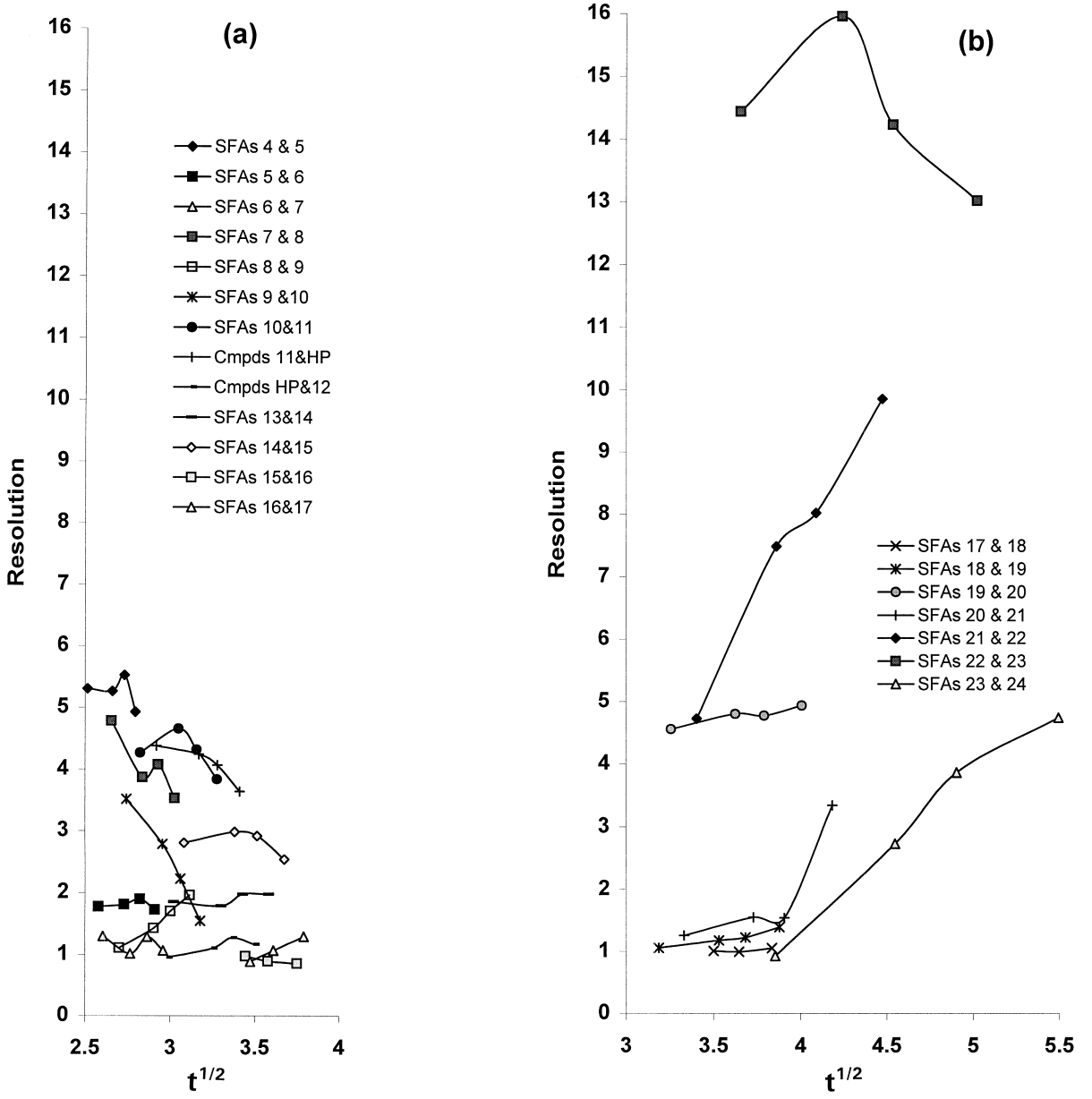

Fig. 8. Resolution plotted versus the square root of the mean analysis time ($t^{1/2}$) for all pairs of compounds. For details see Experimental.

case of SFA pair 20/21 there is a ''hitch'' in the plot. (This is also apparent in Fig. 7 where the resolution of the pair appears not to change between electropherograms b and c). In the other three cases, allowing for some experimental error, R_s is approximately proportional to $\sqrt{t_{app}}$, as predicted by Eq. (3). Again within experimental error, approximately linear increases in R_s are also observed for SFA pairs 18/19, 19/20 and 21/22 in Fig. 4b. For the remainder of the pairs, a variety of shapes of curves are observed.

In an endeavour to maximise the clarity of Fig. 8 we have strung the individual data pieces of each set together rather than draw trend lines. This empha-

sises the experimental scatter in some sets of data, of which there are two principle sources. The first of these is the apparent inconsistency of the electroosmotic mobility (or EOF) in one of the middle concentrations of the buffer and has already been discussed in the previous section. The inconsistency is clear in Fig. 6 in the plot of electroosmotic mobility, is undoubtedly responsible for the slight ''hitch'' in the plots of the electrophoretic mobilities and may be responsible for the ''hitch'' in the plot of R_s versus $\sqrt{t_{app}}$ for SFA pair 20/21, and perhaps for other pairs of analytes. The second significant source of uncertainty arises from the measurement of $w_{1/2}$. There is a clear limit to the extent that electropherograms can be usefully photo-enlarged. The normal baseline noise and the thickness of the expanded lines of the trace are limiting. This leads to an experimental uncertainty of only about 3% for compound 24, but is around 6 to 12% in the middle of the electropherograms and could be of the order of 20 to 30% for the narrow peaks at the start of the electropherograms. However, the significance of these percentages will be somewhat diminished by the consistency of measurement (as opposed to the absolute accuracy). With these factors in mind, it is possible to discuss the general shapes of the plots in Fig. 8 and the factors contributing.

There are at least three factors contributing to the shapes of the R_s versus $\sqrt{t_{app}}$ plots in Fig. 4:

(1) The first factor is diffusional band broadening which was taken into account in the theory section, and which, in the absence of other significant effects, gives rise to Eq. (4).

(2) The second factor is Joule heating and there seems to be no doubt that this will occur under the experimental conditions used in this study [7,19,20]. It has been long understood that with increasing current thermal mixing will eventually set in and available plate numbers will fall below the linear increase expected due to diffusion only so that the efficiency (N) will peak and then decrease. This behaviour is generally discussed as a function of increasing applied voltage (V) in a particular buffer (see for example Ref. [21]) and has been experimentally demonstrated for R_s versus V, for several buffer concentrations by Janini et al. [13], but (a) should logically also apply at a fixed voltage when the buffer concentration is increased. (b) When replotted versus buffer concentration, the Janini et al. data [13] reveals R beginning to curve over in the vicinity of 50–60 mM sodium phosphate buffers, at pH 7, for 15, 20 and 25 kV. Given the similarity of experimental conditions between this study and that [13], and the overlapping of their upper buffer concentration range with the lower end of our range, the combination of considerations (a) and (b) leads us to the expectation of R_s achieving a maximum and perhaps declining in value at the highest ionic strengths (if salt concentrations become high enough). Since it is the increase in buffer concentration that leads to the increase in $\sqrt{t_{app}}$ ($=t^{1/2}$) in Fig. 8, these plots might be expected to display the same behaviour. Many of the plots do exhibit this type of inverted parabolic behaviour.

(3) The third factor that may alter the shape of the plots in Fig. 8 arises from non-ideality; the changes in chemical potentials (activity coefficients) that are the salt effects accompanying the increasing buffer concentration and lead to shifts in the ionisation equilibria of the analytes. The result is selective changes in mobilities and is seen as shifts in the relative positions of analytes in the electropherograms. (This phenomenon has been discussed in detail in Parts II [20] and III [7] of this series of papers and a specific example of changed relativity due to selectively changed ionisation with increasing buffer concentration has been demonstrated [7]). In the current data set, reference to SFAs 8, 9 and 10 in Fig. 7 indicates that whilst R_s is increasing for 8 and 9, it is decreasing at a similar rate for 9 and 10. One explanation for this is that the ionisation of 9 is increasing with salt concentration. The data of Fig. 6 support this in that it is the electrophoretic mobility of 9 that is changing relative to 8 and 10 whilst these two analytes appear to be fixed relative to their neighbours.

From Fig. 8, it is clear that the relative behaviour of pairs of compounds is highly specific, with factors 1–3 above having greatly different effects in different cases.

In an earlier work, Janini et al. [22] produced resolution surfaces as a function of applied voltage (10–25 kV over 50 cm) and buffer concentration (0–50 mM acetate). At low voltages, if we ignore the ''shallow maximum'', R_s appears to vary in a manner similar to the reciprocal of a higher power

with respect to buffer concentration (C). As these authors point out, $t_{app} \propto \sqrt{C}$ under their conditions of experimentation. Combined with Eq. (4), this would predict $R_s \propto C^{1/4}$.

4.3. Selectivity as a function of buffer cation(s)

Fig. 7a was obtained at 65 m*M* potassium phosphate buffer and is generally similar to that obtained for the sodium phosphate buffer at the same concentration [7]. However, there are exceptions.

In the case of the group of compounds 15–19, the selectivity displayed in Fig. 7a in the 65 m*M* potassium phosphate buffer is identical with that observed in the mixed sodium–potassium phosphate buffer in both 30 and 50 m*M* total phosphate [3]. In both cases SFAs 16 (SBE) and 17 (SMOZ) are fused whilst the remainder of the group are largely resolved. In the sodium only phosphate buffer, SFAs 16 and 17 are the best resolved pair and it is 17 (SMOZ) and 18 (SIOX) that are fused in 65 m*M* buffer [7]. By 100 m*M* buffer the five SFAs are largely and uniformly resolved in all cases and the separation appears to be only a function of the total ionic strength (or phosphate concentration in particular).

This similarity of the CZE separations in the potassium only and sodium–potassium buffers appears to be compatible with the work of Salomon et al. [18]. These authors point out that the anomalous EOF in K^+ buffers relative to the other alkali metal ions is due to the preferred adsorption of K^+ ions in the double layer. Thus the presence of K^+ may exert a disproportionate effect on CZE separations in the presence of Na^+.

The other anomaly arises for SDI and SDIM and is contrary to the case above. In the mixed sodium–potassium buffer SDI (13) precedes SDIM (12) and the pair are slightly resolved in 30 m*M* phosphate, largely resolved in 50 m*M* phosphate and unresolved in 100 m*M* phosphate [3]. In the sodium only buffer SDI (13) again precedes SDIM (12) and the pair are largely resolved in 65 m*M* phosphate and unresolved in 101 m*M* phosphate. The behaviour is identical. In the potassium buffer SDIM and SDI comigrate in 65 m*M* buffer (Fig. 7a), but are largely resolved ($R_s \approx$ 1.1) in 174 m*M* buffer (Fig. 7d), albeit in the reversed order of elution to the sodium or mixed buffer. In fact all aspects of the SDIM and SDI separation are inverted between the sodium and potassium buffers; both the order of migration and the effect of increasing buffer concentration are reversed.

The causes of these detailed differences are unknown and are unlikely to be discovered until careful studies of the salt effects upon the ionisation and electrostatic adsorption in the electrical double layer of analytes have taken place.

References

[1] A. Wainwright, J. Microcol Sep. 2 (1990) 166–175.
[2] M.T. Ackermans, J.L. Beckers, F.M. Everaerts, H. Hoogland, M.J.H. Tomassen, J. Chromatogr. 596 (1992) 101–109.
[3] M.C. Ricci, R.F. Cross, J. Microcol Sep. 5 (1993) 207–215.
[4] C.-E. Lin, W.-C. Lin, W.-C. Chiou, E.C. Lin, C.-C. Chang, J. Chromatogr. A 755 (1996) 261–269.
[5] C.-E. Lin, C.-C. Chang, W.-C. Lin, J. Chromatogr. A 759 (1997) 203–209.
[6] C.-E. Lin, C.-C. Chang, W.-C. Lin, J. Chromatogr. A 768 (1997) 105–112.
[7] R.F. Cross, J. Cao, J. Chromatogr. A 818 (1998) 217–229.
[8] K.P. Bateman, S.J. Locke, D.A. Volmer, J. Mass Spectrom. 32 (1997) 297–304.
[9] C.L. Ng, H.K. Lee, S.F.Y. Li, J. Chromatogr. 598 (1992) 133–138.
[10] Q. Dang, Z. Sun, D. Ling, J. Chromatogr. 603 (1992) 259–266.
[11] J.W. Jorgenson, K.D. Lukacs, Anal. Chem. 53 (1981) 1298–1302.
[12] J. Cao, R.F. Cross, J. Chromatogr. A 695 (1995) 297–308.
[13] H.J. Issaq, I.Z. Atamna, G.M. Muschik, G.M. Janini, Chromatographia 32 (1991) 155–161.
[14] I.Z. Atamna, C.J. Metral, G.M. Muschik, H.J. Issaq, J. Liq. Chromatogr. 13 (1990) 2517–2527.
[15] H.J. Issaq, I.Z. Atamna, C.J. Metral, G.M. Muschik, J. Liq. Chromatogr. 13 (1990) 1247–1259.
[16] P. Sandra, presented at Chromatography '94, Sydney, July, 1994.
[17] G.M. Janini, K.C. Chan, J.A. Barnes, G.M. Muschik, H.J. Issaq, Chromatographia 35 (1993) 497–502.
[18] K. Salomon, D.S. Burgi, J.C. Helmer, J. Chromatogr. 559 (1991) 69–80.
[19] J.H. Knox, K.A. McCormack, Chromatographia 38 (1994) 207–214.
[20] R.F. Cross, J. Cao, J. Chromatogr. A 809 (1998) 159–171.
[21] H. Engelhardt, W. Beck, T. Schmitt, in: Capillary Electrophoresis – Methods and Potentials, Vieweg, Wiesbaden, 1996, p. 25.
[22] I.Z. Atamna, H.J. Issaq, G.M. Muschik, G.M. Janini, J. Chromatogr. 588 (1991) 315–320.